Med Glas (Zenica) 2026;23(1)
https://doi.org/10.17392/2080-23-01

Med Glas (Zenica)

ORIGINAL ARTICLE

Von Mises stress analyses using finite element model in two patients with chronic low back pain

Arief Indra Perdana Prasetya[1,2], Tri Indah Winarni[3,4], Jamari Jamari[4,5], Ardiyansyah Syahrom[6,7]

[1]Department of Surgery Sub Orthopaedic and Traumatology, Faculty of Medicine, Universitas Islam Sultan Agung, Semarang, Central Java, Indonesia, [2]Postgraduate Program, Faculty of Medicine, Diponegoro University, Semarang, Central Java, Indonesia, [3]Department of Anatomy, Faculty of Medicine, Diponegoro University, Semarang, Central Java, Indonesia, [4]Undip Biomechanics Engineering and Research Centre (UBM-ERC), Diponegoro University, Semarang, Central Java, Indonesia, [5]Department of Mechanical Engineering, Faculty of Engineering, Diponegoro University, Semarang, Central Java, Indonesia, [6]Department of Applied Mechanics and Design, School of Mechanical Engineering, Universiti Teknologi Malaysia, Johor, Skudai, Malaysia, [7]Mechanical Engineering and Medical Device and Technology Centre (MEDITEC), Universiti Teknologi Malaysia, Johor, Skudai, Malaysia

ABSTRACT

Aim To investigate biomechanical properties of low back pain, which is a pervasive issue with a profound impact on an individual's quality of life due to pain and daily activity limitations.

Methods Two female patients suffering from chronic low back pain were presented. Patient 1 had severe compression fractures at L2 and L4, while Patient 2 had degenerative lumbar scoliosis due to L4-5 disc degeneration. We utilized Finite Element Analysis based on patient-specific CT scan data of lumbosacral 3D reconstruction to quantify the stress intensity as a measurement, known as Von Mises Stress. The reconstruction of the data was performed using specialized software, and simulations were conducted using Ansys 2020. To validate our results, we compared them to previous simulations.

Results Patient 1 exhibited the highest Von Mises stress in the annulus fibrosus at L2-L3 during axial rotation (84.168 MPa) and in the nucleus pulposus at L2-3 during anterior flexion (16.722 MPa). Patient 2 displayed the highest Von Mises stress both in the annulus fibrosus and nucleus pulposus at L1-L2 during axial rotation (0.515 MPa and 0.0594 MPa, respectively).

Conclusion Our findings can help identify the segments at the highest risk for developing lumbar spondylosis and disc degenerative disorders by quantifying Von Mises stress in the lumbosacral region.

Keywords: disc degeneration; finite element analysis; low back pain; lumbosacral spondylosis.

INTRODUCTION

Lumbosacral spine is referred to as the lower segment of the spinal column, consisting of the lumbar vertebrae (L1-L5) followed by the sacrum (S1). The intervertebral discs, which consist of the annulus fibrosus and the nucleus pulposus, are located between each adjacent vertebrae. Spine comprises complex structures such as vertebrae, intervertebral discs, ligaments, and muscles. Degeneration can occur in the intervertebral discs, which can cause pain in the lower back (1,2).

Low back pain (LBP) represents a prevalent issue that significantly impacts quality of life. It is primarily attributed to the considerable discomfort experienced in the lower back, especially the lumbosacral region, and the subsequent impairment in carrying out routine daily activities. Lumbar disc degeneration is a progressive disease that alters the geometric morphology and biomechanical properties, affecting the transmission and allocation of the lumbar spine (2,3). Lumbar disc degeneration can be caused by age, gender, body mass index (BMI), and lumbar load (3). The most common cause of LBP in older individuals is attributed to degenerative processes affecting various components of the spinal column, including each spinal segment, facet joints, intervertebral discs, and the supporting muscles and ligaments of the vertebral column. The degenerative process is caused by compressive forces, commonly known as axial loading, acting upon each segment of the spinal column and intervertebral disc (2,3,4). Understanding the underlying mechanism of lumbar disc degeneration that causes pain is essential when analysing the basic principles of spine biomechanics, developing new surgical methods, and identifying optimal treatment options (1,5).

Numerous analyses of in vitro experiments have been conducted to comprehend the impact of spine biomechanics in disc degeneration. These experiments include bony stress (6), lumbar spine range of motion (ROM) (7), intradiscal pressure

***Corresponding author:** Arief Indra Perdana Prasetya
Department of Surgery Sub Orthopaedic and Traumatology, Faculty of Medicine, Universitas Islam Sultan Agung
Jl. Kaligawe Raya Km.4, Terboyo Kulon, Genuk
Semarang 50112, Central Java, Indonesia
Phone: +6224 6583584
E-mail: ariefindraorthopaedi@students.undip.ac.id
ORCiD ID: https://orcid.org/0000-0002-0513-6201

| Submitted: 19. Sep 2025. Revised: 25. Nov 2025, Accepted: 05. Dec 2025.

(8), and lumbar spine strain rate (9). However, studies relying on experiments are not sufficient, as such tests depend on the availability of specimens and cannot adequately control for different disc degenerative changes. Identifying mechanical differences caused by intervertebral disc degeneration can be simplified and made more accurate using finite element modelling (10-12). By determining the magnitude of von Mises stress obtained in each lumbosacral segment, we can estimate which segments are at the highest risk and can develop into lumbar spondylosis or further disc degenerative disorders.

The aim of this study was to understand the biomechanical properties of lumbar spine in patients suffering from low back pain by determining the von Mises stress using finite element modelling.

PATIENTS AND METHODS

Patients and study design

Two patients who experienced low back pain (LBP) attended to Sultan Agung Hospital in 2022 were presented. Patient 1 is a 62-year-old female who suffered a severe old compression fracture of the second lumbar (L2) and a mild compression fracture of the fourth lumbar (L4) disc. Patient 2 is a 46-year-old female who suffered degenerative lumbar scoliosis due to intervertebral disc L4-5 degeneration.

Both patients underwent 3D reconstruction lumbosacral CT scan and the obtained output was saved as DICOM (Digital Imaging and Communications in Medicine) file. The measured anthropometric parameters were lumbar lordosis, ventral disc height, and dorsal disc height (13). Lumbar lordosis angle was measured by Cobb's method by forming two lines (Figure 1A), i.e. the line drawn perpendicular to lumbar vertebra one upper plate and lumbar vertebra five endplate perpendicular line (14, 15). Ventral disc height (VDH) and dorsal disc height (DDH) (Figure 1B) are the distance between the ventral and dorsal ends of the lumbar disc (13). Measurement was done using mimics 21.0 software with the measure features.

The geometry model was produced from the CT scan data in the form of a DICOM file which then entered the Mimics 21.0 software (Figure 1C and 1D) for the lumbar vertebral bone segmentation process and the smoothing model process, so that the finished model was entered into the Geomagic Studio 12.0 software for the surfacing process (Figure 1E and 1F). SolidWorks 2018 and Design Modeller software were used for the process of making intervertebral discs. For meshing and simulation (Figure 1G and 1H), ANSYS 2020 R1 software was used (2,10,14,16-17).

Methods

The simulation of loading on the first lumbar to the first sacral began by conducting a meshing convergence study. The model lumbar one to sacral one used in this convergence study contained 31 models consisting of six cortical bone, five cancellous bone, five upper endplate, five lower endplate, five annulus fibrosus, and five nucleus pulposus. The element size used in this simulation refers to literature studies that have been carried out and follow research conducted by Kang et al. (18). Material properties on each lumbar vertebral component were from Kang et al. previous research (18). Following that, each

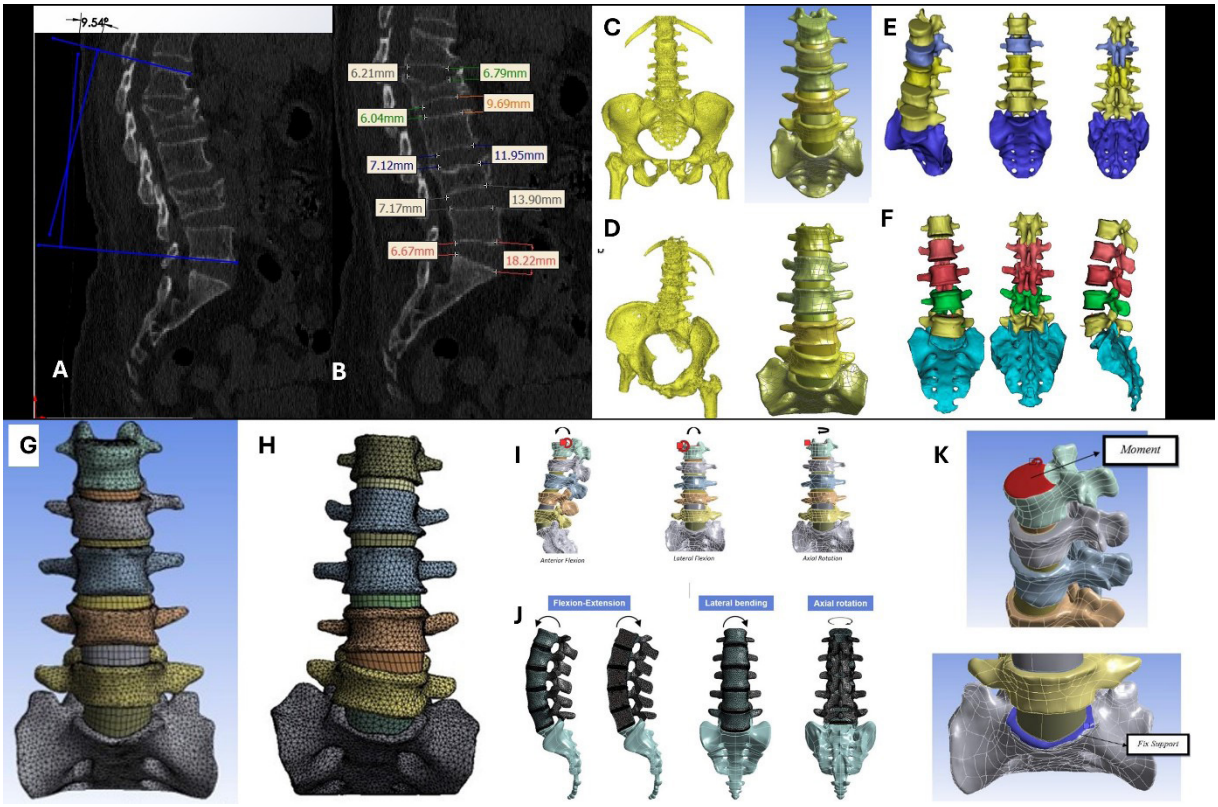

Figure 1. A) Measurement of lumbar lordosis angle; B) Ventral and dorsal disc height measurement; C) Convert geometry model and segmentation process using Mimics 21.0 software in patient 1; D) Convert geometry model and segmentation process using Mimics 21.0 software in patient 2; E) Smoothing and finalization using Geomagic Studio 12.0 software in patient 1; F) Smoothing and finalization using Geomagic Studio 12.0 software in patient 2; G) Meshing process using ANSYS 2020 R1 in patient 1; H) Meshing process using ANSYS 2020 R1 in patient 2; I) Simulation with several loading directions using ANSYS 2020 R1 in patient 1; J) Simulation with several loading directions using ANSYS 2020 R1 in patient 2; K) Moment and fix support location

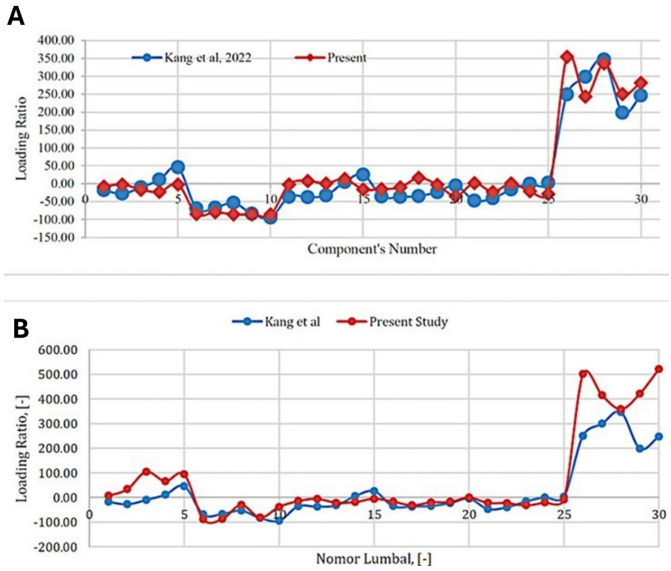

Figure 2. Validation by comparing the result of simulation with Kang et.al simulation. A) showing result for patient 1; B) showing result for patient 2

spinal component was modelled as an isotropic linear-elastic material defined by Young's modulus (representing stiffness) and Poisson's ratio (representing lateral deformation during axial loading) (18). For the validation process, material properties of both normal and osteoporotic bones were used; however, for the subsequent analyses in this study, only the material properties of normal bones were applied.

The loading ratio is a calculation of the ratio of changes in the von Mises stress value between normal bone conditions and bone conditions that experience osteoporosis. The loading ratio calculation was carried out with the formula (A-B)/B x 100%, where A and B stand for the condition of osteoporotic bones and normal bones, respectively (Figure 2).

The load given to the lumbar vertebrae was adjusted to the basic motion in the human lumbar vertebrae (Figure 1I and 1J), namely anterior flexion-extension, lateral bending, and axial rotation (18). The sacrum bone affords fixed support while the upper surface of the lumbar vertebral one cortical bone receives load in the form of motion (Figure 1K).

Statistical analysis

The validation process of the simulation results was determined by comparing the loading ratio findings of the author's simulation with the simulation findings carried out by Kang et al. (18). We used the material properties of each lumbar spine component based on the previous study by Kang et al. (18) (Table 1). Validation using geometric parameters could not be performed because the initial CT data used to reconstruct each lumbosacral segment were obtained from scans conducted at Sultan Agung Islamic Hospital, whereas Kang et al. used a different CT dataset. The original geometric data (e.g., exact vertebral and disc dimensions) from Kang et al. were not available for direct comparison; therefore, one-to-one geometric validation between the two models was not feasible.

Table 1. Material properties of lumbar vertebral component

Components of the lumbar vertebrae	Modulus young (MPA)		Rasio poisson (-)	
	Normal	Osteoporosis	Normal	Osteoporosis
Cortical Bone	12000	8040	0.3	0.3
Cancellous Bone	200	34	0.25	0.25
Endplate	1000	670	0.3	0.3
Nucleus Pulposus	1	9	0.49	0.4
Annulus Fibrosus	4.2	5	0.45	0.45

RESULTS

Based on the lumbar lordotic angle measured using Cobb's method, Patient 1 had a lumbar lordosis of 9.54°, whereas Patient 2 had a lumbar lordosis of 26.50° (Table 2). The loading ratio data obtained from the simulation results of the first lumbar bone to the first sacral bone showed the same trend as the loading ratio reported by Kang et al. (18) (Figure 2).

Computer simulations were performed on both patients from vertebra lumbar one to sacral one with three different loading conditions, with a moment of 400 Nm on the upper surface of lumbar one. Von Mises stress was calculated from the computer simulation result on vertebral body (Figure 3A and 3D), annulus fibrosus (Figure 3B and 3E) and nucleus pulposus (Figure 3C and 3F), respectively.

Table 2. Disc height measurement

Vertebra lumbal	Ventral Disc Height (VDH) (mm)		Dorsal Disc Height (DDH) (mm)	
	Patient 1	Patient 2	Patient 1	Patient 2
L1 – L2	6.79	7.53	6.21	3.22
L2 – L3	9.69	8.32	6.04	3.32
L3 – L4	11.95	8.46	7.12	3.84
L4 – L5	13.90	13.35	7.17	6.01
L5 – S1	18.22	12.06	6.67	5.03

Simulation of Patient 1

Through variations in loading conditions, different maximum points of von Mises stress occurred in the modelling of the lumbar one to sacral one. Under anterior flexion and lateral flexion loading conditions, the maximum von Mises stress point occurred in the upper endplate component of L3-L4 with the von Mises stress value of 391.16 MPa. Under axial rotation loading conditions, the cortical bone component had the highest value of von Mises stress in 172.52 MPa.

The minimum von Mises stress points in the various loading conditions of the modelling of lumbar one to sacral one all occurred in the nucleus pulposus component of L5-S1. Under anterior flexion loading variation, the von Mises stress value in the nucleus pulposus component of L5-S1 is 0.88315 MPa. Under axial rotation and lateral flexion loading variations, the von Mises stress values were 5.4451 MPa and 2.0629 MPa, respectively.

In this study, a three-dimensional simulation was performed to visualise the distribution of von Mises stress on the surfaces of the cortical bone, annulus fibrosus, and nucleus pulposus. The distribution of von Mises stress on the cortical bone surface was evenly spread without any region of stress concentrated in the central area of the cortical bone. The colour contours depicted the formations resulting from different loading conditions on the intervertebral disc, which consists of the annulus fibrosus and nucleus pulposus models. In the nucleus pulposus model with lateral flexion loading variations, it is evident

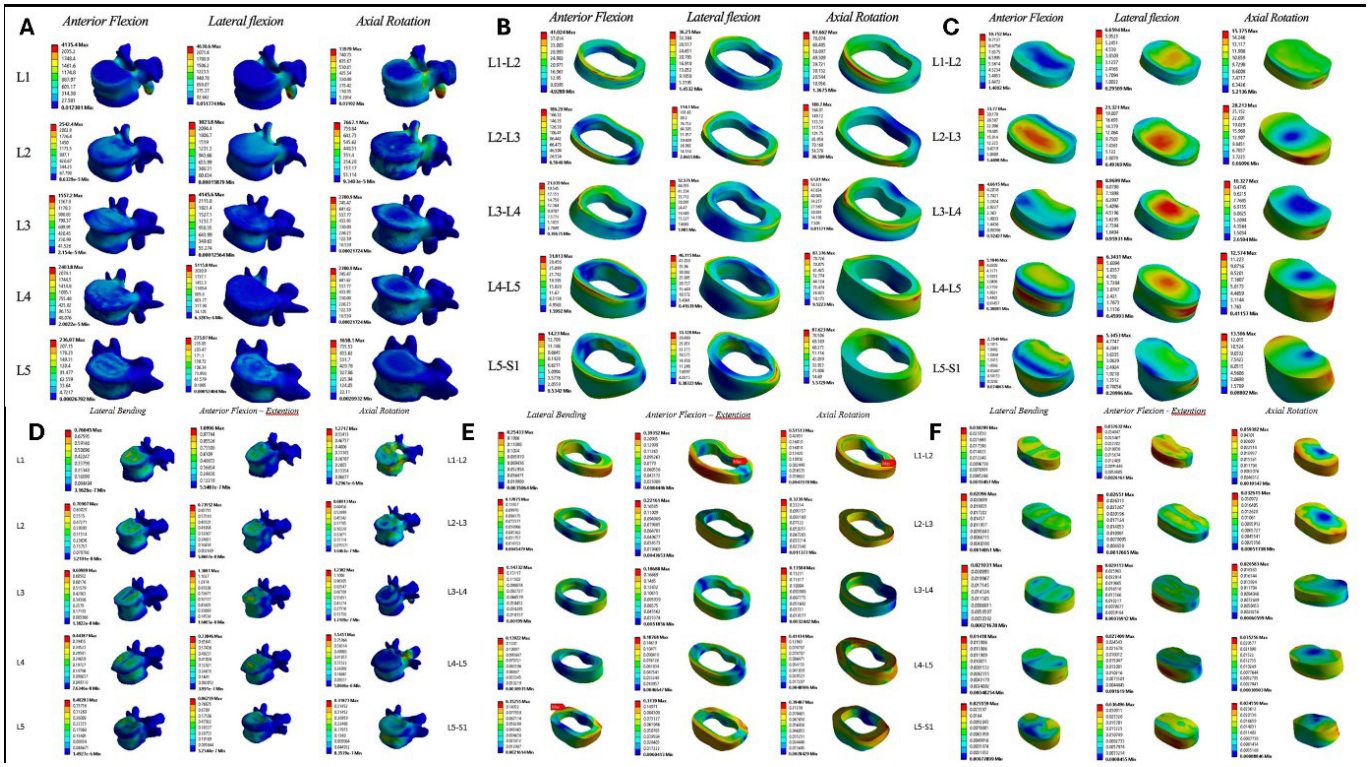

Figure 3. Von Mises stress in patient 1 and 2. A) Von Mises stress of vertebral body patient 1; B) Von Mises stress of annulus fibrosus patient 1; C) Von Mises stress of nucleus pulposus patient 1; D) Von Mises stress of vertebral body; E) Von Mises stress of annulus fibrosus patient 2; F) Von Mises stress of nucleus pulposus patient 2

that in the central region of the L2-3 to L4-5 nucleus pulposus models experienced high von Mises stress. This is indicated by the presence of red colour in the simulation results.

Based on the simulations performed on the modelling of the lumbar one to sacral one in patients, lower back pain attributable to lumbar spondylosis can be observed. The highest von Mises stress on the intervertebral disc for different loading conditions was seen in the annulus fibrosus and nucleus pulposus of L2-L3. The von Mises stress in the annulus fibrosus of L2-L3 is 64.967 MPa under anterior flexion loading, 84.168 MPa under axial rotation loading, and 44.141 MPa under lateral flexion loading. In the nucleus pulposus, the von Mises stress was 16.722 MPa under anterior flexion loading, 12.747 MPa under axial rotation loading, and 10.544 MPa under lateral flexion loading.

Simulation of Patient 2

It was observed that the average value of von Mises stress in the annulus fibrosus and nucleus pulposus components followed the same pattern, with the most significant von Mises stress values occuring in the discs of the lumbar vertebrae L1-L2 under each lateral bending, anterior flexion-extension, and axial rotation loading conditions respectively, were 0.09 MPa, 0.13 MPa, and 0.20 MPa. The von Mises stress values (MPa) for the transient annulus fibrosus for the nucleus pulposus are 0.01 MPa, 0.02 MPa, and 0.02 MPa. Then, the von Mises stress of the annulus fibrosus and nucleus pulposus components on the lumbar intervertebral disc L2-L3 decreases under each loading condition of lateral bending, anterior flexion-extension, and axial rotation loading respectively, were 0.06 MPa, 0.08 MPa, and 0.12 MPa for the annulus fibrosus, while for the nucleus pulposus are 0.009 MPa, 0.012 MPa, and 0.011 MPa. The values of the annulus fibrosus and nucleus pulposus components in the lumbar intervertebral disc L3-L4 also decreased under each condition of lateral bending, anterior flexion-extension, and axial rotation loading conditions are 0.05 MPa, 0.08 MPa, and 0.05 MPa for the annulus fibrosus, and for the nucleus pulposus they are 0.009 MPa, 0.012 MPa, and 0.008 MPa, respectively.

After obtaining the average von Mises stress value, we determined the maximum stress value and location, especially in the annulus fibrosus component, which support the load received by the lumbar vertebrae bone while surrounding and protecting the component in it, namely the nucleus pulposus, which is a gel liquid. Annulus fibrosus that has undergone degeneration (thinning) can cause pain, and worst of all, can suffer damage where it is no longer able to protect the nucleus pulposus, so that when the vertebral bone receives the load of the nucleus pulposus, it can come out through the gap of the fibrosus annulus that has been damaged, or what is commonly called the Hernia Nucleus Pulposus (HNP) (25). This often occurs mainly in the dorsal part of the intervertebral discs. Stress concentration of the annulus fibrosus component is highest in lumbar vertebrae 1-2 when experiencing axial rotation and anterior flexion-extension loads, namely 0.51 MPa and 0.39 MPa. However, for lateral bending stress concentration loads found in the annulus fibrosus vertebra lumbar 5 - sacral 1 is 0.35 MPa. This is due to the patient experiencing degenerative lumbar scoliosis in the lower lumbar vertebrae so that the bone structure becomes asymmetrical but more inclined to the right of the patient. The result of degenerative lumbar scoliosis is also seen when the lumbar vertebral bone experiences axial rotation load, the maximum stress value of the annulus fibrosus is found, which is also significant in the discs of the lumbar 4-5 and the lumbar 5 – sacral 1 are 0.41 MPa and 0.39 MPa. The contour plots of the lumbar vertebrae illustrate both the magnitude of the von Mises stress and the locations of stress concentration within the annulus fibrosus and nucleus pulposus.

DISCUSSION

Simulation analyses of Patient 1

Based on the loading data obtained from the simulations conducted, von Mises stress occurred while the modelling was exposed to variations of lateral flexion loading conditions. The highest von Mises stress value was noted in the upper endplate component of L3-L4 with a von Mises value of 451.46 MPa. The lowest von Mises stress value was noted in the nucleus pulposus component when subjected to anterior flexion loading conditions, with a value of 0.88315 MPa.

Patient 1 suffered an old compression fracture of the second and fourth lumbar, leading to loss of lordosis (9.54º), while the normal range of lumbar lordosis in the adult population measured by Cobb's angle technique is between 40-60º (19). The loss of lumbar lordosis due to an old compression fracture can indeed have an impact on von Mises stress distribution in the spine. Lumbar lordosis refers to the natural curve of the lower spine, which helps to distribute forces and loads evenly throughout the vertebral column during various activities (20). When a vertebral compression fracture leads to a loss of lumbar lordosis, the normal alignment of the spine is disrupted. This altered spinal alignment can put uneven distribution of mechanical loads across the vertebral bodies, discs, and other supporting structures. Therefore, certain spine areas might experience higher stress concentrations, including von Mises stress (21,22). The loss of lumbar lordosis can lead to a more flattened or kyphotic alignment of the spine, which can affect the biomechanics of weight-bearing and movement (19). This change in alignment may cause the vertebral bodies to experience different loading patterns than they would in a healthy spine with the normal lumbar lordosis. Consequently, some regions of the spine may be subjected to higher stress levels due to the changed loading conditions, potentially leading to increased von Mises stress. An old vertebral compression fracture can lead to higher von Mises stress as a result of changes in the mechanical properties of the affected vertebral body (20,22). When a vertebral compression fracture occurs, the structural integrity of the vertebral body is compromised, lowering its capacity to withstand mechanical loads. As the vertebral body heals over time, it may become more rigid and less flexible compared to a healthy vertebral body. This altered mechanical behaviour can result in an uneven distribution of stress during weight-bearing activities. The surrounding areas of the healed fracture site might experience higher stress concentrations, which can lead to an accumulation of stress and ultimately result in higher von Mises stress (20-22) (Figure 3A-C).

Additionally, the altered geometry and biomechanics resulting from the healed fracture can disrupt the natural load distribution within the spine, causing neighbouring vertebral bodies to compensate for the compromised structural integrity. This compensation can further contribute to increased stress on certain regions of the spine, including the area of the old fracture. In summary, an old vertebral compression fracture can lead to higher von Mises stress caused by changes in the mechanical properties of the healed vertebral body, altered load distribution, and potential compensatory mechanisms within the spine (18,23).

Simulation analyses of Patient 2

Current literature indicates that lumbar spondylosis is commonly caused by intervertebral disc degeneration, which is characterized by narrowing of the intervertebral joint space. By looking at the value of the von Mises Stress in the intervertebral disc component, it has been noted that the von Mises stress value of intervertebral disc (annulus fibrosus and nucleus pulposus) has a reciprocal relationship with the value of the lumbar disc height parameter, where the most significant average von Mises stress is found in the discs of lumbar 1-2 with ventral parameters and dorsal disc height values of 7.53 mm and 3.22. The average von Mises stress value of the lumbar vertebra 2-3 disc decreased as far as the ventral parameters and the dorsal disc height increased to 8.32 mm and 3.32 mm. Continuing at the average of the von Mises stress value, the discs of the lumbar vertebrae 3-4 also decreased as many ventral parameters and dorsal disc height increased to 8.46 mm and 8.46 mm (24-26).

Patient 2 suffered from degenerative lumbar scoliosis, which is represented as asymmetry of the lateral curve of the lumbar segment. This condition is caused by disc degenerative disease with uneven load distribution leading to an unequal portion of the disc shape. In degenerative lumbar scoliosis caused by disc degenerative disease, the correlation with von Mises stress is complex and influenced by various biomechanical factors. It is interesting to note that the highest von Mises stress occurs in the upper lumbar region, while the apex of degenerative scoliosis curvature is in the L4-5 region (28,29) (Figure 3D-F).

This phenomenon can be explained by considering the altered biomechanics and load distribution associated with the scoliotic curvature as follows.

Altered alignment. The presence of a scoliotic curve resulting in an abnormal lateral curvature of the spine. This altered alignment shifts the load-bearing dynamics and introduces asymmetrical forces on the vertebral bodies, discs, and facet joints. The spine adapts to this misalignment by redistributing loads across different regions (28,30).

Compensation mechanisms. The spine has an inherent ability to compensate for misalignments. In the case of degenerative lumbar scoliosis with an apex at L4-L5, the upper lumbar region (above the apex) may undergo compensatory changes to maintain overall spinal balance. This can lead to increased stress in the upper lumbar vertebrae, as they work to support the imbalanced forces resulting from the scoliosis curve (28,31).

Changes in load distribution. The scoliotic curvature can cause the vertebral discs to experience uneven loading. The discs in the upper lumbar region might have to bear a larger portion of the load due to the curvature's effects. As a result, the von Mises stress may be higher in these upper lumbar discs, reflecting the increased mechanical demands placed upon them. This condition is synchronous with the condition occurring in Patient 2, where the intervertebral disc at the level L1-2 has less height than other levels (30,31).

Facet joint mechanics. The facet joints are important structures that guide spinal movement and distribute loads. In scoliosis, the facet joints may experience abnormal loading due to the altered alignment. This could increase stress concentrations, especially in regions where the alignment changes (28,29).

The limitations of this study were: Finite Element model used in this research does not include tendons, ligaments, and muscles. Further finite element analyses using a combination of lumbosacral MRI and CT scans are necessary. Hydrostatic pressure was not included in our analysis; therefore, the results of our study reflect changes in overall stress intensity rather than pure compressive–tensile loading. In addition, this study does not account for the anisotropy of bone tissue or the role

of interstitial fluid, which is an important factor in the mechanics of intervertebral discs. Future studies should incorporate these to accurately represent the mechanical response; the load applied in this simulation is based on a reference of 400Nm from a study conducted by Kang et al. Simulation using the patient's body weight as a load can be used to obtain more realistic results, perform finite element analyses involving a larger sample size and a greater variability of lumbar abnormalities; performing finite element analyses utilizing the entire vertebral segment from the cervical to the lumbosacral region.

In summary, the correlation between degenerative lumbar scoliosis and von Mises stress involves complex interactions between altered alignment, compensatory mechanisms, load distribution, and facet joint mechanics. The specific location of the highest von Mises stress (upper lumbar region) can be attributed to the adjustments the spine makes to accommodate the scoliotic curvature and maintain balance. It should be kept in mind that this explanation is a simplified overview, and the actual biomechanics involved can be more intricate and influenced by individual factors. (28-31).

In this study, the reconstruction of vertebra lumbar 1-sacral 1 has been carried out as well as a comprehensive analysis of finite elements for von Mises stress that occurs in the reconstruction results of lumbar 1 to sacral 1. The results of this study can be concluded as follows: finite element modelling can offer a more straightforward and more accurate method of analysis in finding mechanical changes due to lumbar curve alteration and/or intervertebral disc degeneration; patient 1 had an old compression fracture of the second and fourth lumbar, which can lead to higher von Mises stress due to changes in the mechanical properties of the healed vertebral body, altered load distribution, and potential compensatory mechanisms within the spine; patient 2 with degenerative lumbar scoliosis due to disc degenerative disease presents complex interactions between altered alignment, compensatory mechanisms, load distribution, and facet joint mechanics resulting in higher von Mises stress. The specific location of the highest von Mises stress (upper lumbar region) might be attributed to adjustments the spine makes to accommodate the scoliotic curvature and maintain balance; by determining the magnitude of von Mises stress obtained in each lumbosacral segment, we can estimate which segments are at the highest risk, and which can develop into lumbar spondylosis or further disc degenerative disorders.

AUTHOR CONTRIBUTIONS STATEMENT

Conceptualization, A.I.P.P. and A.S.; Methodology, A.I.P.P, and A.S.; Software, A.I.P.P, and A.S.; Validation, T.I.W. and J.J.; Formal Analysis, A.I.P.P. and A.S.; Investigation, A.I.P.P. and A.S.; Resources, T.I.W and J.J.; Data Curation, A.I.P.P. and A.S.; Writing (Original Draft), A.I.P.P.; Writing (Review & Editing), T.I.W., J.J., A.S.; Visualization, A.I.P.P.; Supervision, T.I.W., J.J., and A.S.; Project Administration T.I.W. and J.J.; Funding Acquisition T.I.W. and J.J.

FUNDING

This work was supported by Universitas Diponegoro RPIBT No. 569-186/UN7.D2/PP/VII/2022

TRANSPARENCY DECLARATION

Conflicts of interest: None to declare

REFERENCES

1. Park WM, Kim K, Kim YH. Effects of degenerated intervertebral discs on intersegmental rotations, intradiscal pressures, and facet joint forces of the whole lumbar spine. Comput Biol Med 2013; 43(9):1234–40.
2. Lu X, Li D, Wang H, Xia X, Ma X, Lv F, et al. Biomechanical effects of interbody cage height on adjacent segments in patients with lumbar degeneration: a 3D finite element study. J Orthop Surg Res 2022; 17(1):1–9.
3. Aoki Y, Takahashi H, Nakajima A, Kubota G, Watanabe A, Nakajima T, et al. Prevalence of lumbar spondylolysis and spondylolisthesis in patients with degenerative spinal disease. Sci Rep 2020; 10(1):1–4.
4. Iatridis JC, MacLean JJ, Roughley PJ, Alini M. Effects of mechanical loading on intervertebral disc metabolism in vivo. J Bone Joint Surg Am. 2006;88(Suppl 2):41–6.
5. Cai X, Sun M, Huang Y, Liu Z, Liu C, Du C, et al. Biomechanical effect of L4–L5 intervertebral disc degeneration on the lower lumbar spine: a finite element study. Orthop Surg 2020; 12(3):917–30.
6. Chepurin D, Chamoli U, Diwan AD. Bony stress and its association with intervertebral disc degeneration in the lumbar spine: a systematic review of clinical and basic science studies. Glob Spine J 2021; 12(5):964–79.
7. Wang W, Kong C, Pan F, Wang Y, Wu X, Pei B, et al. Biomechanical comparative analysis of effects of dynamic and rigid fusion on lumbar motion with different sagittal parameters: an in vitro study. Front Bioeng Biotechnol 2022; 10:1–13.
8. Bostelmann R, Steiger HJ, Cornelius JF. Effect of annular defects on intradiscal pressures in the lumbar spine: an in vitro biomechanical study of diskectomy and annular repair. J Neurol Surg A Cent Eur Neurosurg 2017; 78(1):46–52.
9. Li K, Zhang S, Du C, Zhao J, Liu Q, Zhang C, et al. Effect of strain rates on failure of mechanical properties of lumbar intervertebral disc under flexion. Orthop Surg 2020; 12(6):1980–9.
10. Eremina G, Smolin A, Xie J, Syrkashev V. Development of a computational model of the mechanical behavior of the L4–L5 lumbar spine: application to disc degeneration. Materials 2022; 15(19):6684.
11. Masni-Azian N, Tanaka M. Biomechanical investigation on the influence of the regional material degeneration of an intervertebral disc in a lower lumbar spinal unit: a finite element study. Comput Biol Med 2018; 98:26–38.
12. Ding H, Liao L, Yan P, Zhao X, Li M. Three-dimensional finite element analysis of L4–L5 degenerative lumbar disc traction under different pushing heights. J Healthc Eng 2021; 2021:1–9.
13. Hohenhaus M, Volz F, Merz Y, et al. The challenge of measuring spinopelvic parameters: inter-rater reliability before and after minimally invasive lumbar spondylodesis. BMC Musculoskelet Disord.2022; 23(1):1–10.

14. Nan C, Ma Z, Liu Y, Ma L, Li J, Zhang W. Impact of cage position on biomechanical performance of stand-alone lateral lumbar interbody fusion: a finite element analysis. BMC Musculoskelet Disord 2022; 23(1):1–11.
15. Skaf GS, Ayoub CM, Domloj NT, Turbay MJ, El-Zein C, Hourani MH. Effect of age and lordotic angle on the level of lumbar disc herniation. Adv Orthop. 2011;2011:1–6.
16. Shen H, Fogel GR, Zhu J, Liao Z, Liu W. Biomechanical analysis of different lumbar interspinous process devices: a finite element study. World Neurosurg 2019; 127:e1112–19.
17. Zhang M, Ren W, Mo Z, Li J, Pu F, Fan Y. Biomechanics of adjacent segment after three-level lumbar fusion, hybrid single-level semi-rigid fixation with two-level lumbar fusion. Comput Methods Biomech Biomed Engin 2021; 25(4):455–63.
18. Kang S, Park CH, Jung H, Lee S, Min Y, Kim C, et al. Analysis of the physiological load on lumbar vertebrae in patients with osteoporosis: a finite-element study. Sci Rep 2022; 12(1):1–14.
19. Been E, Kalichman L. Lumbar lordosis. Spine J 2014; 14(1):87–97.
20. Matsumoto K, Shah A, Kelkar A, Mumtaz M, Kumaran Y, Goel VK. Sagittal imbalance may lead to higher risks of vertebral compression fractures and disc degeneration—a finite element analysis. World Neurosurg 2022; 167:e962–71.
21. Ye LQ, Liang D, Li Z, Weng R, Huang X, Feng Y, et al. Optimizing cement distribution in the fractured area for osteoporotic vertebral compression fractures through biomechanical effects analysis based on a three-dimensional lumbar finite element model [Internet]. Research Square [Preprint]. 2020 [cited 2025 April 22]. Available from: https://doi.org/10.21203/rs.3.rs-100325/v1
22. Yan J, Liao Z, Yu Y. Finite element analysis of dynamic changes in spinal mechanics of osteoporotic lumbar fracture. Eur J Med Res 2022; 27(1):142.
23. Cui X, Zhu J, Yang W, Sun Y, Huang X, Wang X, et al. Finite element study of sagittal fracture location on thoracolumbar fracture treatment. Front Bioeng Biotechnol 2023; 11:1–12.
24. Skaf GS, Ayoub CM, Domloj NT, Turbay MJ, El-Zein C, Hourani MH. Effect of age and lordotic angle on the level of lumbar disc herniation. Adv Orthop 2011;2011:1–6.
25. Tsujimoto R, Abe Y, Arima K, Nishimura T, Tomita M, Yonekura A, et al. Prevalence of lumbar spondylosis and its association with low back pain among community-dwelling Japanese women. BMC Musculoskelet Disord 2016; 17(1):1–6.
26. Muraki S, Akune T, Oka H, Ishimoto Y, Nagata K, Yoshida M, et al. Physical performance, bone and joint diseases, and incidence of falls in Japanese men and women: a longitudinal cohort study. Osteoporos Int 2012; 24(2):459–66.
27. Pappou IP, Cammisa FP, Girardi FP. Correlation of end plate shape on MRI and disc degeneration in surgically treated patients with degenerative disc disease and herniated nucleus pulposus. Spine J 2006; 7(1):32–8.
28. Rustenburg CME, Kingma I, Holewijn RM, Faraj SSA, Veen A, Bisschop A, et al. Biomechanical properties in motion of lumbar spines with degenerative scoliosis. J Biomech 2019; 102:109495.
29. Zheng J, Yang Y, Cheng B, Cook D. Exploring the pathological role of intervertebral disc and facet joint in the development of degenerative scoliosis by biomechanical methods. Clin Biomech (Bristol, Avon) 2019; 70:83–8.
30. Guo Y, Wang J, Ding J. Degenerative characteristics and biomechanical effects of paravertebral muscles in patients with degenerative lumbar scoliosis. Chin J Postgrad Med 2021; 825–31.
31. Haddas R, Hu X, Lieberman IH. The correlation of spinopelvic parameters with biomechanical parameters measured by gait and balance analyses in patients with adult degenerative scoliosis. Clin Spine Surg 2020; 33(1):E33–9